Driving forces for Ag-induced periodic faceting of vicinal Cu(111)

A. R. Bachmann,[1,2,*] S. Speller,[2] A. Mugarza,[3] and J. E. Ortega[3,4]

[1] *Fachbereich Physik, Universität Osnabrück, Barbarastrasse 7, 49069-Osnabrück, Germany*
[2] *Nijmegen Research Institute of Materials, University of Nijmegen, Toernooiveld 1, 6525 ED Nijmegen, The Netherlands*
[3] *Departamento de Física Aplicada I, Universidad del País Vasco, Plaza de Oñate 2, E-20018 San Sebastian, Spain*
[4] *Donostia International Physics Center and Centro Mixto CSIC/UPV, Manuel Lardizabal 4, 20018-San Sebastian, Spain*

(Dated: February 1, 2008)

Adsorption of submonolayer amounts of Ag on vicinal Cu(111) induces periodic faceting. The equilibrium structure is characterized by Ag-covered facets that alternate with clean Cu stripes. In the atomic scale, the driving force is the matching of Ag(111)-like packed rows with Cu(111) terraces underneath. This determines the preference for the facet orientation and the evolution of different phases as a function of coverage. Both Cu and Ag stripe widths can be varied smoothly in the 3-30 nm range by tuning Ag coverage, allowing to test theoretical predictions of elastic theories.

Self-organization on crystal surfaces is a promising alternative for growing uniform nanostructures with regular sizes and spacings [1, 2]. In the case of one-dimensional nanostructures one can use the regular step arrays of vicinal surfaces as templates. Ideally atomic steps are preferential adsorption sites, and wires and stripes can be grown by step-flow. However, if the terrace width increases to a few nanometers, single steps tend to meander and their spacing becomes irregular. Yet vicinal surfaces offer another alternative at this mesoscopic scale, i.e. using adsorbates to induce the formation of periodic facets, which are much stiffer than individual steps. In this case the miscut angle as well as the adatom concentration can be tuned to obtain a variety of stripe patterns that are potential templates for further nanostructure growth [3, 4, 5, 6, 7]. The fundamental problem is controlling this complex process in order to predict and obtain useful template structures. Therefore it is important to understand the microscopic mechanisms that determine the stripe pattern formation.

In the atomic scale, the driving force of the adsorbate-induced faceting appears to be the lattice matching of the adsorbate layer with a particular substrate orientation. The high step density of the vicinal surface facilitates the step bunching and the formation of facets with better lattice matching in the direction perpendicular to the steps. Thus at a temperature where both adatom and surface step mobilities are high enough the system breaks up into two phases, namely well-matched adsorbate-covered facets and adsorbate-free stepped stripes. A widely studied case is Au on vicinal Si (v-Si). Here a variety of overlayer reconstructions match to different Si crystal planes, leading to a family of striped patterns made of low symmetry facets and wide (111) or (100) terraces with different Au concentrations [3, 4, 5]. The final morphology depends on the total amount of Au deposited, the temperature and the vicinal angle of the clean surface. Furthermore, one can tune miscut angle and Au coverage to obtain a well-matched single phase system [4]. More recently adsorbate-induced faceting and nanostructuration has been observed for Ag and NaCl on v-Cu(111) [6, 7]. In these cases the lattice matching is good between Ag(111) and Na(100) packed layers and Cu(112) and Cu(223) planes, respectively. This induces stripe patterns of covered and uncovered facets, as well as changes in the facet orientation as a function of coverage.

The important question concerns the mesoscopic scale, i.e. the nanostructure periodicity. Using the elastic theory of continuous media for two-phase systems Marchenko has shown that the difference in stress between the two phases produces long-range interactions, leading to periodic domain patterns [8]. Although this theory explains well the spontaneous faceting of clean surfaces [9], or the coverage-dependent periodicity of adsorbate patterns on flat surfaces [10], it is an open question whether it can be applied for adsorbate-induced faceting. On one hand, because the growth of strained layers might bring in other types of elastic relaxations, thereby suppressing the characteristic wavelength [11]. On the other hand, the adsorbate-induced faceting is a more complex process that involves huge mass transport and restructuration of two different chemical species, and hence it is more likely to be kinetically restricted. This is the case of Au/v-Si(100) and NaCl/v-Cu(111) [7, 12]. Here we analyze the Ag-induced faceting of v-Cu(111). We show that this self-assembled striped structure can be tuned in the 3-30 nm range by simply controlling Ag coverage [13]. The morphology of the system is stable over a wide temperature range. At the atomic scale we show that faceting is driven by the tendency of Ag to form (111)-like packed layers with minimum stress. At the mesoscopic scale we are able of proving, for the first time in adsorbate-induced faceting, the coverage-dependent periodicity predicted by the continuum elastic theory at thermal equilibrium.

The substrate is v-Cu(111) with 11.8° miscut about

the $[\bar{1}\bar{1}2]$ direction. The surface preparation is described elsewhere [6]. Ag deposition was done with the substrate held at 300K. The regular stripe structure is produced after subsequent annealing to 420K. Further annealing to 700K does not produce any appreciable change in Scanning Tunneling Microcopy (STM) images or Low Electron Diffraction (LEED) patterns, strongly suggesting thermal equilibrium. In order to have a continuous variation of the coverage, Ag is deposited as a wedge. The coverage is calculated from STM images using 3000 Å^2 frames and assuming that Ag covered areas consist of packed, 1 monolayer (ML) thick patches. Such assumption is consistent with the structural analysis of Ag-covered areas and also with Auger Electron Spectrocopy measurements [6].

In Figures 1 (a) to 1 (e) we study the morphology of the system as a function of Ag coverage by means of STM and LEED. Fig. 2 schematically depicts the side view of the faceted structure deduced from the analysis. The clean surface shows a regular array of monoatomic, {100}-like steps along the $[\bar{1}10]$ direction, giving rise to the characteristic spot splitting in LEED. The average terrace width measured with both LEED and STM is d=10.2 Å, i.e. the surface mostly shows (223)-like terraces ($4\frac{2}{3}$ atomic rows per terrace, d=10.5 Å) with a few (335)-like terraces ($3\frac{2}{3}$ atomic rows, d=8.4 Å). As shown in Figs. 1(b)-(d), upon Ag adsorption the system undergoes faceting. Below 1 ML we distinguish three different regimes, which differ on the crystallographic orientation of the Ag-covered facet. These are the A-regime up to ∼0.52 ML, the B-regime between ∼0.52 ML and ∼0.76 ML, and the C-regime from ∼0.76 ML to 1 ML.

Figs. 1 (b)-(c) correspond to the A-regime, which is characterized by a fairly regular hill-and-valley structure of Ag-covered facets oriented in the (112) direction and clean Cu stepped areas. The inset of Fig. 1 (b) shows a closer view of the surface, where we can observe the Moire pattern in the Ag-covered facet, and monoatomic steps at clean Cu stripes with their typical frizzy edges. In the LEED pattern we have both the spot structure from the Ag Moire and the splitting from the step array in the Cu stripe. As observed in Figs. 2 (b)-(c) and depicted in Fig. 2, increasing the Ag coverage in A-regime results in a higher density of Ag-covered stripes and a reduction of the step density at clean Cu bands. The latter is due to the fact that Cu(112) facets (d=6.25 Å, $2\frac{2}{3}$ atomic rows per terrace) have higher step density than the average surface, thus their relative growth requires additional steps from Cu stripes. Such effective step removal from Cu stripes is nicely followed in the LEED pattern in Fig. 1 (e). The Cu splitting smoothly shrinks as a function of Ag coverage, and both spots merge into a single one with 0.52 ML, when A-regime saturates [14].

The B-regime from 0.52 ML to 0.76 ML is characterized by a smooth transition in the Ag-covered facet orientation from (112) to (335). The latter is closer to the surface normal, allowing a higher Ag saturation. (335)-covered areas develop directly from the center of preexisting (112) facets or arise by melting two contiguous (112) facets. In both cases, the (335) orientation characterizes the center of the Ag-covered stripes, whereas the boundaries preserve the (112) orientation. For 0.72 ML in Fig. 1 (d) the B-regime is almost saturated, i.e. we have flat Cu(111) terraces and mostly (335)-oriented Ag stripes, also displaying a Moire structure. During the C-regime, from 0.76 ML to 1ML, (223) facets develop. With 1 ML we observe a close-packed Ag layer wetting a random distribution of (335)- and (223)-like terraces with the same step density than the starting surface.

In the atomic scale, the driving force for the Ag-induced faceting of the stepped Cu surface is the matching between Ag(111)-like packed rows along the parallel direction of the steps and the Cu facet underneath. Lattice-matching has been also proposed as the microscopic mechanism for the NaCl-induced faceting of Cu(112) [7]. Our system generally displays a clear tendency to avoid adsorption on wide (111) terraces, which leads to a large mismatch [15]. On the other hand, as deduced from Figs. 1 and 2, there is a preference for (112)-oriented facets at low coverages, in spite that this requires a larger mass transport. This can be naively explained from the width of the Cu terrace required for a good matching in the perpendicular direction. Five Ag packed rows (2.498 Å wide each) fit to two 6.25 Å wide terraces in Cu(112) with only 0.12% mismatch in the direction perpendicular to the steps, whereas Cu(335) requires two 8.37 Å wide terraces to accommodate seven Ag rows with 4.47% mismatch. This preference for (112) facets is also supported by the microscopic analysis of (112) and (335) stripes shown in Fig. 3. The atomic models in the right panels of Fig. 3 reproduce the Moire patterns of the left panels in the simplest way. The open circles represent Ag-close packed layers, the small dots the Cu(112) and Cu(335) unit cell underneath, and the shades the "on-top" positions. Thus, in this simple approach the step corrugation is being disregarded. We use the smallest compressions and azimuthal rotations of the Ag(111) adlayer to obtain the Moires that fit to the STM observations. For both (112)- and (335)-oriented layers the Ag layer rotation is the same 5.2°, allowing the smooth transition from (112) to (335) facets observed beyond 0.52 ML. For (112) facets the Ag adlayer is compressed by 0.5% and 7.8% in the direction perpendicular and parallel to the rows, respectively. For (335) facets the perpendicular and parallel compressions are 6.2% and 7.8%, respectively. Thus, the (335)-oriented layer accumulates much more stress, explaining the preference to form (112)-oriented stripes.

The long range periodicity of the Ag-induced faceting of Fig. 1 is nicely explained within Marchenko's elastic theory, as shown in Fig. 4. Data points represent the nanostructure period (L) and the Ag stripe width (w_{Ag})

measured from the STM images as a function of coverage (θ) from 0.1 ML to 0.9 ML. The periodicity is poorly defined above 0.52 ML, and in this case we consider the average value $\langle L\rangle$, defined as $\langle L\rangle = \langle w_{Ag}\rangle + \langle w_{Cu}\rangle$, where $\langle w_{Ag}\rangle$ and $\langle w_{Cu}\rangle$ respectively are the average widths of Ag-covered facets and Cu stripes. The lines in Fig. 4 are fit to the data using Marchenko's model, where the superlattice periodicity L and the stripe width w_{Ag} are given by [8]:

$$L(\theta) = \frac{\kappa}{\sin(\pi\theta)} \quad ; \quad w_{Ag}(\theta) = \frac{\kappa\theta}{\sin(\pi\theta)} \qquad (1)$$

κ is the only adjustable parameter. The model is strictly defined for a two-phase system, and hence the fit is restricted to the A-regime. The result is excellent and we obtain $\kappa_A = 91\pm6$ Å. Data points at regime transitions display a clear discontinuity. Microscopically, this appears related to the way some new facets develop, i.e. by melting two contiguous facets in the previous regime. But, as indicated in Fig. 4, by changing in Eq. 1 to κ_B= 110±8 Å and κ_C= 141 ±8 Å both $\langle w_{Ag}(\theta)\rangle$ and $\langle L(\theta)\rangle$ in B- and C-regimes are still nicely reproduced.

In Marchenko's approach κ is related to elastic constants via $\kappa = 2\pi\ a \times \exp(1 + C_1/C_2)$, where a is a microscopic cutoff and C_1 is the free energy of the phase boundary per unit length [8]. If we assume that work function variations between Cu and Ag phases are relatively small [10], C_2 has only elastic nature and reflects the stress difference between phases [8]:

$$C_2 = \frac{1-\nu^2}{\pi E}\ |\vec{F}|^2 \qquad (2)$$

where E and ν respectively are the shear modulus and the Poisson ratio for Cu, and $\vec{F} = (\vec{\sigma}_{Ag} - \vec{\sigma}_{Cu})$ the force exerted at facet edges due to the difference in surface stress between Ag-covered facets and Cu stripes, as defined in the inset of Fig. 4. The general agreement with Marchenko's theory shown in Fig. 4 indicates that κ in Eq. 1 does not have a significant coverage-dependence. The θ-dependence is expected in the elastic constants due to the changing shape of Cu stripes and Ag-covered facets. Even with coverage-dependent elastic constants Eq. 1 always holds if there is a (relatively) high stress energy in any of the Ag-covered facets, such that $C_1/C_2 \sim 0$. The actual value of C_1/C_2 can be obtained from the fit in Fig. 4 assuming a cutoff length a. The cutoff length is defined as the minimum size of the (growing) domain [10, 16], which in this context is the terrace width. Using $\kappa_A = 91\pm2$ Å and a=6.25 Å, we indeed obtain C_1/C_2= -0.15 ± 0.05. The absolute value of C_1/C_2 is thus much smaller than any other found in the literature, and can be assumed to be zero [17]. The condition $C_1/C_2 \sim 0$ is expected to hold for B and C regimes as well. The boundary energy must be very similar, because the atomic structure at facet edges is the same in all regimes, whereas the stress difference is expected to increase, since the preference for (112) orientation indicates that the lowest surface energy occurs for this facet. Thus only a change in a would explain the changes in κ in Fig. 4. The discontinuities in Fig. 4 are in fact consistent with the increasing terrace size (cutoff a) of the growing facet. The fitting parameter variation from κ_A = 91 Å to κ_B= 110 Å (21%) and to κ_C= 141 Å (28%) closely correlates with the relative increase in the terrace size from d_{112}=6.25 Å to d_{335}=8.4 Å (34%) and to d_{223}=10.5 Å (25%). Since κ discontinuities were microscopically related to melting of contiguous facets at regime transitions, this makes the real nature of the cutoff length an interesting issue that encourages a detailed microscopic model.

Note that the $C_1/C_2 \sim 0$ case leads to the shortest possible superlattice period in Ag/v-Cu(111). This contrasts with the long superlattice periods observed at high temperatures in NaCl/v-Cu(111) [7]. Long periods are only possible if $C_1/C_2 \gg 1$, which in the latter case could be due to a more efficient interface relaxation, favored by a large adsorbate-surface charge transfer that weakens Cu-Cu bonds.

A.R.B. and S.S. are supported by the Deutsche Forschungsgemeinschaft (DFG) and the Stichting voor Fundamenteel Onderzoek der Materie (FOM). A.M. and J.E.O. are supported by the Universidad del País Vasco (1/UPV/EHU/00057.240-EA-8078/2000)and the Max Planck Research Award Program. Fruitful discussions with A. Rubio are acknowledged.

* Corresponding author. Electronic address: andreas.bachmann@physik.uni-osnabrueck.de

[1] J. Hannon et al., Science **295**, 299 (2002); R. Plass et al., Nature **412**, 875 (2001).
[2] V. A. Shchukin et al., Rev. Mod. Phys. **71**, 1125 (1999).
[3] L. Seehofer et al., Surf. Sci. **329**, 157 (1995); K. Aoki et al., Surf. Sci. **408**, 101 (1998);H. Minoda et al., Surf. Sci. **432**, 69 (1999).
[4] F. J. Himpsel et al., J. Phys. Condens. Matt. **13**, 1 (2001).
[5] H. Minoda et al., Phys. Rev. B **59**, 2363 (1999); M. Horn von Hoegen et al., Surf. Sci. **433-435**, 475 (1999).
[6] A. R. Bachmann et al., Phys. Rev. B **64**, 153409 (2001).
[7] S. Fölsch et al., Phys. Rev. Lett **84**, 123 (2000); S. Fölsch et al., Surf. Sci. **497**, 113 (2002).
[8] V. I. Marchenko et al., Sov. Phys. JETP **52**, 129 (1980).
[9] S. Rousset et al., Surf. Sci. **422**, 33 (1999).
[10] D. Vanderbilt, Surf. Sci. **268**, L300 (1992); Kwok-On Ng et al., Phys, Rev. B **52**, 2177 (1995).
[11] J. Tersoff et al., Phys. Rev. Lett. **75**, 2730 (1995); F. Liu et al., Phys. Rev. Lett. **80**, 1268 (1998).
[12] Frank-J. Meyer zu Heringdorf et al., Phys. Rev. Lett **86**, 5088 (2001).
[13] This makes Ag/Cu system very attractive to tailor sur-

face states (A. R. Bachmann et al. (unpublished)).
[14] *A*-regime ideally saturates at 0.61 ML, when Cu stripes become flat (111) terraces [6]. However some steps appear pinned by defects within Cu stripes, such that the effective saturation coverage is lower.
[15] I. Meunier et al., Phys. Rev. B **59**, 10910 (1999).
[16] F. K. Men et al., Phys. Rev. Lett. **88**, 96105 (2002).
[17] . With such a small C_1/C_2 ratio, the negative sign, which is not physical, must be attributed to the elastic model limitations.

FIG. 1: (a)-(d) STM images and (e) (0,0) LEED spot measured at different coverages for Ag-induced faceting in vicinal Cu(111). Up to 0.6 ML, the system displays periodic, two-phase separation of Ag-covered (112) facets and clean Cu stepped stripes. Both give distinct LEED structures in (e), i.e. spot splitting for Cu stripes and Moiree pattern spots for Ag facets. As the Ag coverage increases from (a) to (c), steps from Cu stripes incorporate in Ag facets, such that Cu terraces become wider. This is proved by the splitting reduction in (e). (335) facets like those in (d) develop beyond 0.6 ML.

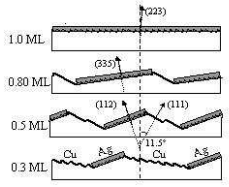

FIG. 2: Schematic evolution of the periodic faceting induced by Ag on vicinal Cu(111) with 11.8° miscut, as deduced from the STM-LEED analysis in Fig. 1.

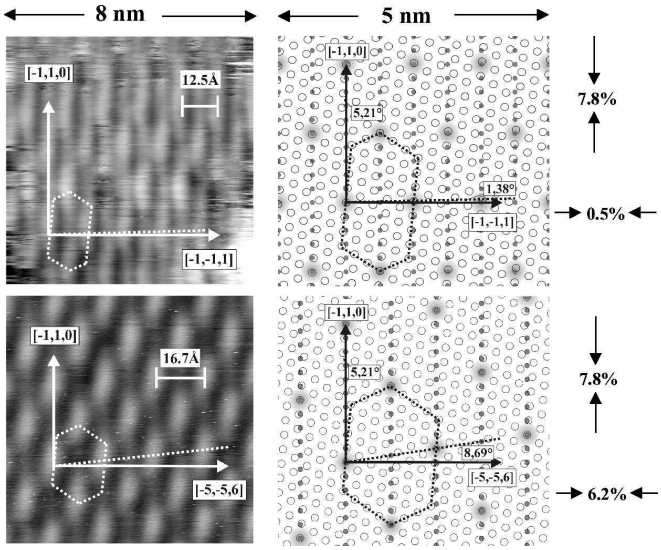

FIG. 3: Left, detailed STM view of the Moiree patterns for (112) and (335) Ag-covered facets. Right, two-dimensional atomic models that reproduce the Moirees in the left. The small filled circles indicate the step edge Cu atom positions underneath. Open dots represent Ag atoms and shaded circles indicate "on-top" positions. The fit requires the indicated compressions and azimuthal rotations of the Ag packed layer.

FIG. 4: Nanostructure periodicity (filled squares) and Ag-covered stripe width (open circles) as a function of Ag coverage. Vertical lines distinguish the A, B and C regimes, which differ on the type of the growing Ag-covered facet. The thick solid lines are fit to the data in the two-phase A-regime using the continuum elastic theory of Marchenko's [8]. A continuation in the $B - C$ regimes is represented by the thin dotted line. The thin solid lines do fit separately data points in the B and C regime. The inset shows the surface stress vectors in a faceted structure (see the text)